DEVELOPMENT OF METHODOLOGIES FOR THE ESTIMATION OF THERMAL PROPERTIES ASSOCIATED WITH AEROSPACE VEHICLES

NASA Grant No. NAG-1-1507
May 1, 1993 - March 31, 1996

A FINAL REPORT

To The Attention Of

Dr. Steve Scotti
Thermal Structures Branch, Mail Stop 396
NASA Langley Research Center
Hampton, Va 23665

By

Elaine P. Scott
Associate Professor
Department of Mechanical Engineering
Virginia Polytechnic Institute and State University
Blacksburg, VA 24061-0238
Phone: (540)231-3940
Fax: (540)231-9100

June 13, 1996

TABLE OF CONTENTS

DEVELOPMENT OF METHODOLOGIES FOR THE ESTIMATION OF THERMAL PROPERTIES ASSOCIATED WITH AEROSPACE VEHICLES

Elaine P. Scott
Department of Mechanical Engineering
Virginia Polytechnic Institute and State University
Blacksburg, VA 24061-0238

1. INTRODUCTION

A thermal stress analysis is an important aspect in the design of aerospace structures and vehicles such as the High Speed Civil Transport (HSCT) at the National Aeronautics and Space Administration Langley Research Center (NASA-LaRC). These structures are complex and are often composed of numerous components fabricated from a variety of different materials. The thermal loads on these structures induce temperature variations within the structure, which in turn result in the development of thermal stresses. Therefore, a thermal stress analysis requires knowledge of the temperature distributions within the structures which consequently necessitates the need for accurate knowledge of the thermal properties, boundary conditions and thermal interface conditions associated with the structural materials.

The goal of this proposed multi-year research effort was to develop estimation methodologies for the determination of the thermal properties and interface conditions associated with aerospace vehicles. Specific objectives focused on the development and implementation of optimal experimental design strategies and methodologies for the estimation of thermal properties associated with simple composite and honeycomb structures. The strategy used in this multi-year research effort was to first develop methodologies for relatively simple systems and then systematically modify these methodologies to analyze complex structures. This can be thought of as a building block approach. This strategy was intended to promote maximum usability of the resulting estimation procedure by NASA-LaRC researchers through the design of in-house experimentation procedures and through the use of an existing general purpose finite element software.

2. SPECIFIC OBJECTIVES

To achieve the overall research goal to develop estimation methodologies for the determination of the thermal properties and interface conditions associated with aerospace vehicles, the research tasks were divided into three phases; each lasting approximately one year. Specific objectives were then formulated for each of these phases. These objectives are outlined below for each phase.

In the first phase, the efforts were primarily directed towards the estimation of thermal properties in isotropic materials, with some limited efforts towards the analysis of anisotropic materials; the stated objectives for the first phase were to

1.1 develop methodologies, including optimal experimental procedures, for the estimation of the thermal properties of isotropic materials at room temperature, and

1.2 extend these methodologies for the estimation of the thermal properties of anisotropic materials in two orthogonal planes.

In the second phase, the efforts were primarily directed towards the estimation of thermal properties in anisotropic materials; here, the stated objectives were to

2.1 develop and implement methodologies, including optimal experimental designs, for the estimation of the thermal properties of anisotropic materials,

2.2 initiate the development of methodologies for the estimation of temperature dependent thermal properties, and

2.3 initiate the development of methodologies for the determination of thermal interface conditions between adjacent structural components.

The final phase of work built on the previous efforts with additional efforts directed towards the analysis of honeycomb sandwich structures. The stated objectives for this phase were to

3.1 implement the procedure for the estimation of in-plane thermal properties, using optimal experimental parameters,

3.2 develop methodologies for the estimation of thermal contact resistance for fastened structures,

3.3 continue the development of optimal experimental design strategies, and

3.4 develop methodologies for the determination of effective and mode-dependent thermal properties of sandwich structures.

3. METHODS AND ACCOMPLISHMENTS

The methods used to meet the stated objectives and the resulting accomplishments are outlined below. The methods and results for the analysis of isotropic and the one dimensional analysis of anisotropic materials, including optimal experimental design and experiments at elevated temperatures, are presented in Sections 3.1 and 3.2, respectively, while the methods and results for the two dimensional analysis of anisotropic materials are presented in Sections 3.3. and 3.4, respectively. The methods used to design experiments and estimate radiative and conductive properties of honeycomb sandwich structures are presented in Section 3.5, while the results are given in Section 3.6. Efforts to estimate contact resistance are presented in Section 3.7, and finally, the development of new optimal design strategies, based on genetic algorithms, are presented in Section 3.8.

3.1 Estimation of Thermal Properties - One Dimensional Analysis

The estimation of the thermal properties using a one dimensional analysis included an estimation procedure, a mathematical model, and experimental measurements. Prior to conducting the experiments, the experimental parameters were optimized. An overview of the methods used to perform these tasks is presented in the following subsections. Many of the details of this work can be found in the progress report by Scott and Moncman (1994).

3.1.1 Estimation Procedure

The methodology used to estimate the thermal properties is based on the minimization of an objective function containing experimental and calculated temperatures with respect to the unknown thermal properties, thermal conductivity and volumetric heat capacity. This procedure is called the Gauss method. The Box-Kanemasu procedure is a modification of this method which can facilitate convergence in some cases; a detailed discussion of the method is given by Beck and Arnold (1977). In the Gauss method, the objective function is the least squares function, S, where

$$S = [\boldsymbol{Y}-\boldsymbol{T}(\boldsymbol{b})]^T[\boldsymbol{Y}-\boldsymbol{T}(\boldsymbol{b})] \tag{1}$$

The matrix $\boldsymbol{Y}$ contains experimental temperatures, and the matrix $\boldsymbol{T}(\boldsymbol{b})$ contains calculated temperatures at corresponding times and locations. The vector $\boldsymbol{b}$ contains the unknown parameters to be estimated. In the estimation procedure, the objective function is minimized with respect to the unknown parameters in $\boldsymbol{b}$. This procedure can be implemented by differentiating Eq. (1) with respect to $\boldsymbol{b}$, setting the resulting expression equal to zero, and then solving for $\boldsymbol{b}$ as shown below.

$$\boldsymbol{b} = [\boldsymbol{X}^T\boldsymbol{X}]^{-1}\boldsymbol{X}(\boldsymbol{Y}-\boldsymbol{T}) \tag{2}$$

where the matrix $\boldsymbol{X}$ is called the sensitivity matrix, and it is defined as

$$\boldsymbol{X} = \nabla_b \boldsymbol{T}^T \tag{3}$$

This matrix is important in that it indicates the sensitivity of the temperature response with respect to changes in a given parameter.

The temperatures contained in $\boldsymbol{Y}$ are obtained from experiments involving a heater which imposes a heat flux at the boundary of a sample, and the calculated temperatures contained in the

vector T are determined from a mathematical model of the experimental system. Descriptions of both the mathematical model and the experimental procedures are found in the following subsections.

3.1.2 One Dimensional Mathematical Model

The formulation of the mathematical model was based on the experimental system being analyzed, and the model consisted of a set of equations from which temperature was determined. In the one dimensional case, the solution to these equations was formulated both analytically and numerically. The numerical solution involved the use of the finite element code Engineering Analysis Language (EAL, Whetstone, 1983). The code has been and continues to be used by researchers in the Thermal Structures Branch at NASA-LaRC, and therefore, the utilization of this existing software has the advantage that NASA-LaRC researchers are already familiar with the code, and thus, enhancing the usability of the resulting parameter estimation software.

In the mathematical model, one-dimensional heat transfer was considered through a thin plate with an aspect ratio such that the two-dimensional heat transfer effects at the edges could be ignored. One plane boundary was considered to be at a known constant temperature, and a heat flux was imposed at the second plane boundary. The heat flux boundary condition was necessary for the independent estimation of thermal conductivity and volumetric heat capacity.

The temperature distribution within the material was determined from conservation of energy:

$$\frac{\partial}{\partial x}\left(k_{eff}\frac{\partial T}{\partial x}\right) = C_{eff}\frac{\partial T}{\partial t} \qquad 0 < x < L \qquad t > 0 \qquad (4)$$

where T is temperature, k_{eff} and L are the effective thermal conductivity and the thickness, respectively, in the direction of heat transfer, x, C_{eff} is the effective volumetric heat capacity (or the product of density and specific heat), and t is time. The heat flux and temperature boundary conditions, along with the initial condition can be described as

$$-k_{eff}\left.\frac{\partial T}{\partial x}\right|_{x=0} = q(t) \qquad x = 0 \qquad t > 0 \qquad (5a)$$

$$T(x,t) = T_b(t) \qquad x = L \qquad t > 0 \qquad (5b)$$

$$T(x,t) = T_0 \qquad 0 \le x \le L \qquad t = 0 \qquad (6)$$

where the heat flux, $q(t)$, the temperature at $x = L$ ($T_b(t)$), and the initial temperature, T_i, are known.

3.1.3 Basic Experimental Set Up for One Dimensional Analysis

The basic experimental apparatus for the one-dimensional case consisted of a thin resistance heater positioned between two (nearly) identical samples and copper blocks placed on the opposite sides of the samples. In this symmetrical set up, the heater was used to provide the heat flux boundary condition, and the copper blocks were used to provide approximate constant temperature boundary conditions. Thermocouples were positioned between the heater and the samples to measure the temperatures required for the estimation procedure. Thermocouples were also placed between the sample, copper block interfaces to determine the temperature boundary condition.

3.1.4 Optimal Experimental Design - Methods

The basic experimental design described above requires selection of the experimental parameters, including the heating time, temperature sensor location, and total experimental time. Prior to conducting the experiments, an optimization procedure was used to determine the experimental parameters required for an optimal experimental design. The objective here was to develop an optimal experimental design which would produce temperature measurements which would provide the smallest confidence regions for the estimated thermal properties.

The first step in the optimization procedure was to define an optimization criterion. Recall that the objective of the experiment was to minimize the confidence regions of the resulting property estimates. This can be accomplished through the maximization of the sensitivity of the temperature measurements with respect to the unknown thermal properties. The criterion used in this study is called the *D*-criterion; the objective here is to maximize the dimensionless determinant, D^*, of the $\mathbf{X}^{*T}\mathbf{X}^*$ matrix, which contains the products of the dimensionless sensitivity coefficients. These coefficients indicate the sensitivity of the temperature response with respect to a given parameter and were obtained by differentiating temperature with respect to the unknown parameter. The dimensionless sensitivity coefficients used in this study are given by

$$X_1^* = \frac{k_{eff}}{q_o L/k_{eff}} \frac{\partial T}{\partial k_{eff}} \tag{7}$$

and

$$X_2^* = \frac{C_{eff}}{q_o L/k_{eff}} \frac{\partial T}{\partial C_{eff}} \tag{8}$$

where T, k_{eff}, C_{eff}, and L were defined previously, and q_0 is a nominal heat flux.

Once the sensitivity coefficients were determined, the dimensionless determinant for the case of two parameters was found from (Beck and Arnold, 1977):

$$\begin{aligned} D^* &= |\mathbf{X}^{*T}\mathbf{X}^*| \\ &= d_{11}^* d_{22}^* - (d_{12}^*)^2 \end{aligned} \tag{9a,b}$$

where

$$d_{ij}^* = \left[\frac{1}{T_{\max}^{*\,2}}\right]\left[\frac{1}{m t_N^*}\right] \sum_{p=1}^{m} \int_0^{t_N^*} X_i^*(t^*) X_j^*(t^*) dt^* \tag{10}$$

Here, m is the number of temperature sensors used, and t^*, t_N^* and T_{max}^* are defined as

$$t^* = \frac{k_{eff} t}{C_{eff} L^2} \qquad t_N^* = \frac{k_{eff} t_N}{C_{eff} L^2} \qquad T_{max}^* = \frac{(T_{max} - T_i)}{q_0 L/k_{eff}} \tag{11a,b,c}$$

where t_N is the total experimental time, and T_{max} is the maximum temperature reached between the start and end of the experiment, and T_i is the initial temperature.

3.2 Estimation of Thermal Properties - One Dimensional Results

The results from the one dimensional analysis included the optimization of the experimental design and the estimation of the thermal properties of composite and Pyrex samples as functions of temperature.

3.2.1 Optimal Experimental Design - Results

The first optimal experimental parameter determined was the sensor location. The dimensionless determinant was determined for a number of different sensor locations and several different heating times. It was found that the determinant was maximized when the sensor was located at the heated surface ($x^+ = 0.0$) for all heating times. This result was expected since the maximum sensitivity coefficients for both properties occurred at the heated surface.

The next experimental parameter that was determined was the optimal heating time. This was obtained by calculating the dimensionless determinant, D^+, analytically as a function of the total experimental time, t_N^+, for various dimensionless heating times, t_h^+. Here, the heat flux was assumed constant over t_h^+ and zero for $t > t_h^+$. A number of different dimensionless heating times were analyzed, and the optimal heating time was determined from the case producing the largest dimensionless determinant. It was found from this analysis that the optimal dimensionless heating time, $t_{h,opt}^+$, is 2.2 for the basic experimental design considered here. However, it was also found that the magnitude of the dimensionless determinant changed little between dimensionless heating times of 2.0 and 2.5. Therefore, any values within this range will be close to the optimal value and will provide similar results in the estimation procedure.

The last parameter that was determined was the optimal experimental time. In order to see the effect of added data to the value of the determinant, D^+, the determinant was calculated from Eqs. (9) and (10), but without averaging the integral contained in Eq. (10) over time. The results indicated that after a dimensionless time of approximately five, the determinant no longer changed significantly. This implies that after this dimensionless time, the temperatures are reaching steady state and little additional information is being provided for the estimation of the thermal properties. Therefore, the experiments can be concluded after a dimensionless time, t_N^+, of approximately four to five. Note that to be conservative, a value of five was chosen in the experimental studies.

In summary, the optimal experimental parameters found were $x^+ = 0.0$, $t_{h,opt}^+ = 2.2$, and $t_N^+ = 5$.

3.2.2 Estimation Thermal Properties - One Dimensional Results

Several sets of experiments were performed assuming a one dimensional analysis. Each of these are described in the following subsections.

3.2.2.1 IM7/5260 Composite Samples - Results at Room Temperature

Experiments were first conducted at room temperature using the experimental set-up described in Section 3.1.3 and continuous IM7 graphite fiber, Bismaleimide epoxy matrix (IM7/5260) composite samples, each approximately 6.8 mm thick. Based on the dimensionless

optimal experimental parameters presented in Section 3.2.1, the sensors were placed next to the heated surface, the heating time was set equal to 180 seconds, and a total experimental time equal to approximately 500 seconds was used. The experiment was performed three times using the same samples and with voltage inputs to the heater of 4.9V, 6.1V, and 7.3V, resulting in maximum temperature rises of approximately 2°C, 3°C, and 4.5°C. These experiments were performed at NASA Langley Research Center in the Thermal Structures Branch Laboratories.

The measured temperatures obtained from these experiments were then used in the estimation procedure to determine the thermal conductivity perpendicular to the fiber axis and the volumetric heat capacity. The thermal properties were estimated using both an analytical mathematical model and a finite element model (using EAL) to calculate the temperatures in the estimation procedure. The results for the three experiments using the two different mathematical models are given in Table 1, along with their mean and 95% confidence interval for the analytical model. Note that there was very little different between the solutions obtained using the analytical model and EAL. To determine how accurately the calculated temperatures matched the measured temperatures, the Root Mean Square (RMS) error was computed, where

$$RMS = \sqrt{\sum_{i=1}^{n_t} (Y_i - T_i)^2 / n_t} \tag{12}$$

Here, T_i and Y_i are the calculated and measured temperatures, respectively, at the ith time step, and n_t is the total number of temperature measurements. The *RMS* values were calculated two different ways. First the measured temperatures for each individual experiment were compared with calculated values using the thermal properties estimated for that experiment; these values are indicated by RMS_I in Table 1. The *RMS* values were then determined using the experimental temperatures and temperatures calculated using the mean thermal properties values (also shown in Table 1); these values are indicated by RMS_M.

3.2.2.2 IM7/5260 Composite Samples - Results at Elevated Temperatures

Additional experiments were conducted using the IM7/5260 composite samples at elevated temperatures at NASA-LaRC. The samples were used in the basic experimental set-up as described previously with the exception that the entire set-up was placed in an oven, and experiments were conducted at four different initial temperatures ranging from room temperature to approximately 125°C. Three experiments were conducted at each temperature. The measured temperatures obtained from these experiments were then used in the estimation procedure to determine the thermal conductivity and volumetric heat capacity. The results of these tests are shown in Table 2. Good repeatability was found between tests at the same initial temperature, and both thermal conductivity and heat capacity were found to increase with temperature. The thermal conductivity was found to increase approximately 12% from 20°C to 125°C, while the volumetric specific heat increased approximately 28% over the same temperature range.

Table 1. Estimated effective thermal conductivity, k_{eff}, and volumetric heat capacity, C_{eff}, from Experiments 1, 2, and 3, along with the Root Mean Square error calculated from individual and mean thermal property estimates (RMS_I and RMS_M).

	Exp. 1		Exp. 2		Exp. 3		Mean	
	Analytical	EAL	Analytical	EAL	Analytical	EAL	Analytical	EAL
k_{eff} (W/m°C)	0.519	0.518	0.504	0.503	0.529	0.516	0.517±0.023	0.516
C_{eff} (MJ/m³°C)	1.425	1.420	1.505	1.495	1.498	1.467	1.48±0.081	1.467
RMS_I (°C)	0.0526		0.0815		0.0652			
% Max. Temp. Rise	0.24%		0.36%		0.26%			
RMS_M (°C)	0.0548		0.0908		0.0827			
% Max. Temp. Rise	0.34%		0.40%		0.34%			

Table 2. Estimated Thermal Conductivity, k, for Composite Samples MJS92C6 and MJS92C7 Using Symmetrical Stacking Arrangement (E. P. Scott, at LaRC, August 4, 1994).

File Name	Initial Temperature (°C)	k (W/m°C)	C (MJ/m³°C)
943A	20.	0.568	1.50
943B	20.	0.573	1.54
943C	21.	0.570	1.57
943D	49.	0.590	1.59
943E	50.	0.580	1.73
943F	50.	0.580	1.76
943G	89.	0.603	1.80
943H	88.	0.607	1.80
943I	89.	0.607	1.80
943J	124.	0.633	1.98
943K	125.	0.633	1.98
943L	125.	0.647	1.96

3.2.2.3 Pyrex Samples - Results at Elevated Temperatures

A set of experiments was conducted over the same temperature range using a Pyrex standard. These experiments were also performed at the NASA-LaRC Thermal Structures Branch. The experimental set-up was identical except that the samples were 2.4 cm thick. Since the optimal heating time is based partly on the dimensions of the samples, the optimal heating times were much longer than those required for the Pyrex samples (32 minutes compared with 1.5 minutes). Once again, experiments were conducted over a temperature range from room temperature to approximately 125°C, using several different initial temperatures. These results are shown in Table 3. The thermal conductivity was found to increase approximately 17% over the temperature range tested, while the volumetric heat capacity increased approximately 13%. Note that the variability in the estimates from experiments at the same initial temperature was much higher than previously observed with the composite samples. One possible problem was that the oven used did not maintain a constant temperature, and due to the long testing time with these samples, this could have had some influence. It is desired to repeat these tests using another oven. The heat capacity values have a higher variability than the thermal conductivity values because, as shown in the previous reports, the sensitivity is higher for thermal conductivity. These results were compared with estimates for thermal conductivity provided by the manufacturer. A bias was present in the estimates for thermal conductivity; all are approximately 12-13 percent higher than the values provided by the manufacturer. One explanation for this could be that two dimensional effects were present due to the thickness of the samples provided.

3.2.2.4 IM7/5260 Composite Samples - Results from Unsymmetrical Analysis

Another set of experiments was performed at NASA-LaRC using the IM7/5260 composite samples and a modified experiment designed to simulate the estimation of thermal properties from data obtained from a large structure. Here, a resistance heater was placed on top of a composite sample, and the exposed surface of the heater was well insulated, forming an unsymmetrical stacking arrangement. Experiments were then conducted from room temperature to approximately 130°C with at least three tests at four different initial temperatures. The results are shown in Table 4. The thermal conductivity values were less than five percent lower than the estimates using the symmetrically stacked samples, thus indicating that this type of design has a good potential for use in estimating properties in large structures.

Table 3. Estimated Thermal Conductivity, k, for Pyrex Samples (E. P. Scott at LaRC, July 20, 1994).

File Name	Initial Temperature (°C)	k (W/m°C)	C (MJ/m^3°C)
942A	21.	1.30	1.93
942B	23.	1.27	1.82
942C	19.	1.22	1.89
942E	62.	1.33	1.78
942F	51.	1.29	1.81
942H	90.	1.37	1.84
942I	91.	1.27	2.24
942K	107.	1.39	1.94
942L	107.	1.40	1.88
942M	106.	1.47	1.90
942N	118.	1.49	2.07
942O	117.	1.43	1.99
942P	115.	1.41	1.94
942Q	126.	1.50	2.12
942R	126.	1.48	2.10
942S	126.	1.47	2.16
942J	131.	1.49	2.05

Table 4. Estimated Thermal Conductivity, k, for Composite Samples MJS92C6 and MJS92C7 Using Unsymmetrical Stacking Arrangement (E. P. Scott, at LaRC, August 4, 1994).

File Name	Initial Temperature (°C)	k (W/m°C)	C (MJ/m^3°C)
944A	21.	0.571	1.65
944B	21.	0.562	1.50
944C	21.	0.562	1.62
944D	21.	0.563	1.61
944E	21.	0.558	1.64
944I	51.	0.551	1.72
944J	51.	0.560	1.71
944K	51.	0.549	1.67
944L	91.	0.577	1.93
944M	90.	0.570	1.88
944N	91.	0.575	1.93
944F	129.	0.605	2.17
944G	129.	0.604	2.09
944H	130.	0.614	2.10

3.3 Estimation of Thermal Properties - Two Dimensional Analysis

The two dimensional analysis was conducted using procedures similar to the one dimensional analysis described in Section 3.1. In this case, the analysis was directed towards composite samples, and the thermal conductivity parallel and perpendicular to the fiber axis of the composite sample and the volumetric heat capacity were sought. Therefore, three properties were sought simultaneously rather than two. A summary of the analysis and the methods used to perform these tasks are presented in the following subsections. Details of this work can be found in the progress report by Scott and Hanak (1995).

3.3.1 Estimation Procedure

The methodology used to estimate the thermal properties in the two dimensional analysis is the same as that used for the one dimensional analysis described in Section 3.1.1. In using this methodology, it should be noted that the properties sought should be uncorrelated; that is, the sensitivity coefficients need not be linear or near linear dependent. This was found to be a critical factor as discussed in Section 3.4.

3.3.2 Two Dimensional Mathematical Model

In the two dimensional analysis, both analytical and numerical mathematical models were used. The analytical model was first used to optimize the experimental design, and then the numerical model was used in estimating the thermal properties. In each case, two different configurations were considered. The first consisted of an imposed heat flux perpendicular to the fiber axis over a portion of one boundary (with the remainder of the boundary insulted) and known constant temperatures at the remaining three boundaries. The second configuration also has a heat flux imposed over a portion of one boundary, only this time, the boundary opposite to the heat flux is maintained at a constant temperature, while the remaining two boundaries are insulated. Both configurations are shown in Fig. 1.

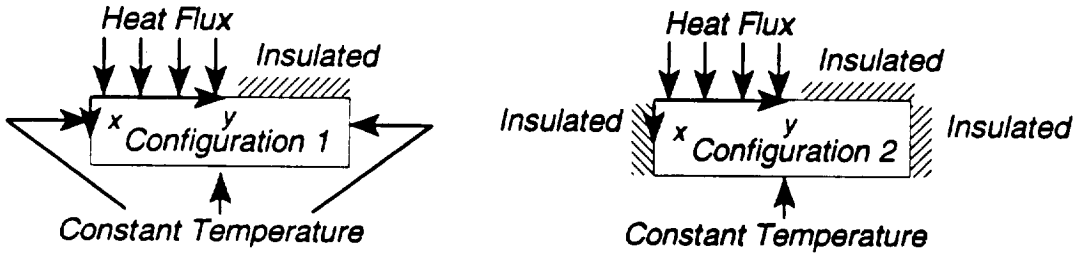

Figure 1. Two-dimensional Boundary Conditions.

In both configurations, the temperature distribution within the material can be determined from conservation of energy:

$$\frac{\partial}{\partial x}\left(k_{x\text{-}eff}\frac{\partial T}{\partial x}\right) + \frac{\partial}{\partial y}\left(k_{y\text{-}eff}\frac{\partial T}{\partial y}\right) = C_{eff}\frac{\partial T}{\partial t} \quad 0<x<L_x \quad 0<y<L_y \quad t>0 \tag{12}$$

where $k_{Y\text{-}eff}$ and y are the effective thermal conductivity and position, respectively, perpendicular to the direction of heat transfer. The boundary conditions can be described by

$$\begin{aligned} -k_{x\text{-}eff}\frac{\partial T}{\partial x} &= q_x && x=0 \quad 0<y<L_p \quad 0<t\le t_h \\ &= 0 && x=0 \quad 0<y<L_p \quad t>t_h \\ &= 0 && x=0 \quad L_p<y<L_y \quad t>t_h \end{aligned} \tag{13}$$

$$T(x, y, t) = T_i \qquad 0<x<L_x \quad 0<y<L_y \quad t=0 \tag{14}$$

$$\frac{\partial T}{\partial x} = 0 \qquad x=0 \quad 0<y<L_y \quad t>0 \tag{15a}$$

$$T(x, y, t) = T_{0,x} \qquad x=L_x \quad 0<y<L_y \quad t>0 \tag{15b}$$

The boundary conditions along the y-axis are for the first configuration are

$$T(x, y, t) = T_{0,y1} \qquad 0<x<L_x \quad y=0 \quad t>0 \tag{16a}$$

$$T(x, y, t) = T_{0,y2} \qquad 0<x<L_x \quad y=L_y \quad t>0 \tag{16b}$$

while the boundary conditions at the same locations for the second configuration are

$$\frac{\partial T}{\partial y} = 0 \qquad 0<x<L_x \quad y=0 \quad t>0 \tag{17a}$$

$$\frac{\partial T}{\partial y} = 0 \qquad 0<x<L_x \quad y=L_y \quad t>0 \tag{17b}$$

The analytical solution was based on the use of Green's functions. This resulted in a double series containing both transient and steady state terms. To increase computational efficiency, the steady state terms, which only needed to be determined once for each run, were determined separately.

The numerical finite element model was formulated using EAL. It was found in conducting the experiments, that the "constant temperature" boundary conditions were not exactly constant. Therefore, temperature measurements from thermocouples placed at the location of the "constant temperature" boundary conditions were incorporated into the finite element code.

3.3.3 Basic Experimental Set Ups for Two Dimensional Analysis

Two basic experimental apparatuses were used for the two-dimensional case. Both consisted of a thin resistance heater positioned between two (nearly) identical samples and aluminum blocks

placed on the opposite sides of the samples. Unlike the one dimensional case, the heat flux was only applied to a portion of the sample. The edges of the composite were insulated on two opposite sides to maintain two dimensional heat transfer. The remaining two edges were either placed in contact with two aluminum blocks which acted as heat sinks for the constant temperature boundary condition (configuration 1) or insulated (configuration 2).

3.3.4 Optimal Experimental Design - Methods

The basic experimental designs described above requires selection of the experimental parameters, including the heating time, heating area, temperature sensor location along both x and y axes, and total experimental time. Prior to conducting the experiments, these experimental parameters were optimized to produce temperature measurements which would provide the smallest confidence regions for the estimated thermal properties. Once again, the D-criterion and the optimization methodology discussed in Section 3.1.4 were used. A two-phase parametric study was used to optimize the parameters. The first phase included determining the general range of the optimal values, while the second phase narrowed this range to determine the values more precisely. The procedure was iterative in that after the general range was determined, one parameter was varied while the others were held constant. Once the value of that parameter with the highest determinant was found, the process was repeated with the next parameter. The entire sequence was then repeated with the updated parameter values on the next iteration.

3.4 Estimation of Thermal Properties - Two Dimensional Results

The results from the two dimensional analysis included the optimization of the experimental design and the estimation of the thermal properties of the composite samples.

3.4.1 Optimal Experimental Design - Results

The first optimal experimental parameter determined was the sensor location along the x^+ axis, parallel to the heat flow. Once again, the optimal location was found to be at the heated surface ($x^+ = 0.0$). Then, the sensor location along the y^+ axis, perpendicular to the heat flow, was determined. The optimal location for configuration 1 was found to be at $y^+ = 0.15$, while the optimal location for configuration 2 was found to be at $y^+ = 0$.

The next experimental parameter that was determined was the optimal heating time. This was obtained by calculating the dimensionless determinant, D^+, analytically as a function of the total experimental time, t_N^+, for various dimensionless heating times, t_h^+. Here, the heat flux was assumed constant over t_h^+ and zero for $t > t_h^+$. It was found from this analysis that the optimal dimensionless heating time, $t_{h,opt}^+$, for both configurations is 1.40. A related experimental parameter is the heating area. In this case the optimal heating area for configuration 1 was over the entire surface, that is $L_p^+ = 1.0$, while for configuration 2, the optimal area was found to be $L_p^+ = 0.15$. Finally, a conservative optimal dimensionless total experimental time was found to be equal to 4.0. It should be noted that using the respective optimal values, the dimensionless determinant for configuration 1 was found to be slightly higher than that for configuration 2, indicating that slightly better estimates could be found using configuration 1.

3.4.2 Estimation of Thermal Properties

The effective thermal conductivity parallel and perpendicular to the fiber axis and the effective volumetric heat capacity were sought in this analysis. The one concern was due to the possible correlation apparent between the two thermal conductivities parallel and perpendicular to the fiber axis. Therefore, prior to estimating these properties with experimental data, the procedure was first tested with simulated data.

The mathematical model was used to generate temperatures which were in turn used in the estimation procedure to obtain the property values which ideally would be equal to the input values used in the mathematical model. This is a common procedure used to assess estimation procedures. At first, exact data were used; that is, no experimental errors were added to the data obtained from the model. All three original thermal properties were obtained from the estimation procedure using exact data, verifying that the process was possible in the best scenario. However, it was also found that very high correlation existed between the two conductivity values, as expected.

Experiments were then performed using configuration 1 and the optimal experimental parameters. The property estimates were again sought; this time with experimental data. Unfortunately, the solution did not converge using the Box-Kanemasu procedure. This indicated that an improved estimation procedure was needed which could handle correlation between the parameters. This has been the focus of additional efforts as noted in Section 3.8. In the meantime, an effort was made to estimate simultaneously the thermal conductivity parallel to the fiber axis and the volumetric heat capacity, given the thermal conductivity perpendicular to the fiber axis from the one dimensional analysis.

Prior to conducting experiments to estimate $k_{y,eff}$ and C_{eff}, the experimental designs for configurations 1 and 2 were re-optimized for the estimation of only these two properties. The optimal experimental parameters for configuration 1 were found to be $x^+ = 0.0$, $y^+ = 0.15$, $t_h^+ = 1.45$, and $L_p^+ = 0.30$, and the optimal parameters for configuration 2 were found to be $x^+ = 0.0$, $y^+ = 0.0$, $t_h^+ = 1.65$, and $L_p^+ = 0.13$. These values had to be adjusted slightly because heaters were not feasibly available at either of the optimal heating areas found. Therefore, the experiments were re-optimized with the heating area fixed at the closest available heater size. The adjusted values were found to be $x^+ = 0.0$, $y^+ = 0.15$, $t_h^+ = 1.35$, and $L_p^+ = 0.25$ for configuration 1, and $x^+ = 0.0$, $y^+ = 0.15$, $t_h^+ = 1.65$, and $L_p^+ = 0.11$ for configuration 2. In this case, the dimensionless determinant for configuration 1 was found to be almost twice as large as that for configuration 2, indicating that if only these two properties are sought, it is a much better experimental design to use.

Once the optimal experimental designs were determined, experiments were first conducted to estimate $k_{y,eff}$ and C_{eff}. Nine experiments were performed using the optimal experimental parameters from three separate experimental set ups each repeated three times. Additional experiments were performed to verify the optimization procedure using non-optimal experimental parameters. The confidence intervals of the resulting estimates were then compared with those obtained using optimal values. First, experiments were conducted using dimensionless heating times associated with dimensionless determinants (D^+) equal to 20% and 80% of the maximum value. This resulted in non-optimal heating times equal to 0.75 and 0.29 for configuration 1 and 0.88 and 0.32 for configuration 2. The second parameter analyzed was the sensor location along the y-axis. The non-optimal heating times used here were $y^+ = 0.05$ and $y^+ = 0.23$ for configuration 1 and y^+

= 0.09 and y^+ = 0.15 for configuration 2. The last experimental parameter to be analyzed was the heating area. The non-optimal values selected in this case were L_p^+ = 0.50 and L_p^+ = 0.75 for configuration 1 and L_p^+ = 0.25 and L_p^+ = 0.75 for configuration 2.

The resulting means of the estimates of $k_{y\text{-}eff}$ and C_{eff} from the nine experiments performed with each set of the optimal and non-optimal experimental parameters are shown in Table 5. Several observations can be noted from these results. First, based on the confidence regions, the optimal designs provided the most accurate combined property estimates. Note also that an individual property might be estimated with greater accuracy at a non-optimal setting, but the combination of properties maintained a higher accuracy at the optimal settings. Furthermore, configuration 1 supplied more information, and therefore, was a better experimental design than configuration 2. Finally, the sensor location was found to the most sensitive experimental parameter investigated; therefore, it is important that the sensors not be placed away from the optimal location.

Table 5. Estimated Mean Values for the In-Plane Thermal Conductivity, $k_{y\text{-}eff}$, and Volumetric Heat Capacity, C_{eff}, from Configurations 1 and 2.

Experimental Parameters		Configuration 1		Configuration 2	
		$k_{y\text{-}eff}$ (W/mK)	C_{eff} (MJ/m^{3}K)	$k_{y\text{-}eff}$ (W/mK)	C_{eff} (MJ/m^{3}K)
Optimal Values		1.89±0.04	1.53±0.01	2.00±0.04	1.56±0.04
Non-optimal heating time,	t_h^+ = 0.75[1], 0.88[2]	1.78±0.06	1.48±0.02	1.88±0.10	1.60±0.05
	t_h^+ = 0.29[1], 0.32[2]	1.54±0.06	1.43±0.02	1.62±0.05	1.56±0.03
Non-optimal sensor location,	y^+ = 0.05[1], 0.09[2]	2.15±0.05	1.98±0.03	2.61±0.06	1.67±0.02
	y^+ = 0.23[1], 0.15[2]	1.99±0.13	1.48±0.03	6.63±0.21	1.52±0.03
Non-optimal heating area,	L_p^+ = 0.50[1], 0.25[2]	2.05±0.05	1.61±0.03	1.64±0.06	1.54±0.01
	L_p^+ = 0.75[1,2]	2.04±0.05	1.55±0.02	2.19±0.04	1.44±0.02

1: Configuration 1; 2: Configuration 2

3.5 Estimation of Thermal Properties of Honeycomb Sandwich Structures - Analysis

A titanium honeycomb core sandwich structure was analyzed assuming one dimensional heat transfer and conductive and radiative heat transfer to estimate both conductive and radiative properties. A summary of the analysis and the methods used to perform this analysis are presented in the following subsections. Details of this analysis can be found in the progress report by Scott and Copenhaver (1996).

3.5.1 Estimation Procedure

Initially, the methodology used to estimate the thermal properties in this analysis was the same as that used for the one dimensional analysis described in Section 3.1.1. In using this methodology, it should be noted that the properties sought should be uncorrelated; that is, the sensitivity coefficients need not be linear or near linear dependent. This was found to be a critical factor; therefore, a constrained optimization method called the Exterior Penalty Function method was used instead.

This strategy was used because it is relatively simple incorporate into the optimization process. It treats the objective function as an unconstrained function but provides a penalty to limit constraint violations. The imposed penalty is initially small but increases with each iteration in order to prevent ill-conditioning. This process requires the solution of several unconstrained problems in order to obtain the optimum constrained problem. Again, details of the procedure can be found in Scott and Copenhaver (1996).

3.5.2 Mathematical Model of the Honeycomb Structure

In this analysis, one dimensional heat transfer was sought through the thickness of the honeycomb core material. Figure 2 shows a schematic of the heat transfer model. A heat flux was assumed on one side of the sample while the other side was assumed to be at a constant temperature or insulated. The side edges were also assumed insulated. A preliminary analysis at steady state indicated that the significant modes of heat transfer were due to conductance through the webs of the honeycomb structure and radiation heat transfer within the interior of each core element for the temperatures under consideration. A finite element model using EAL was formulated using a lumped capacitance model for the face sheets and diffuse, gray body in the interior of the core. Note that the conductance through the air in the interior of the core was neglected. The core material consisted of Ti-6Al-4V titanium, and the face sheets consisted of an aluminum/boron composite.

Since the specific heat and thermal conductivity of core material, Ti-6Al-4V, are well known, these properties were not estimated. The most important feature of the core is the wall thickness which varied due to the fabrication process; therefore, this was estimated instead of the thermal properties of the core material. In addition the emissivity within the core cell was sought, along with the capacitance of the face sheet.

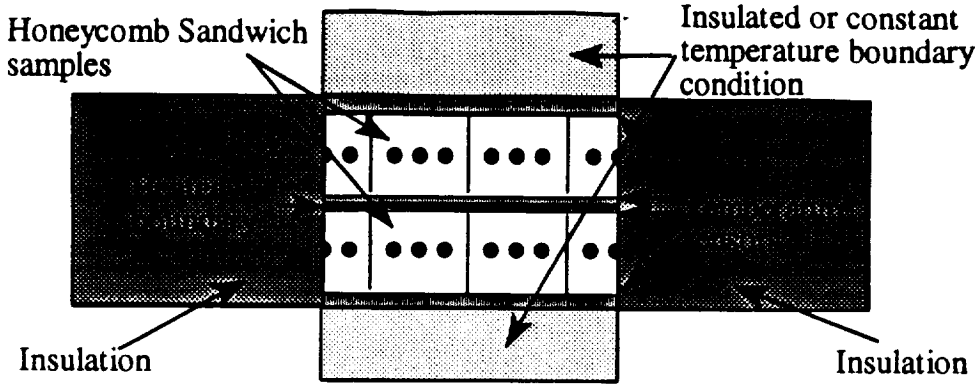

Figure 2. Schematic of Honeycomb Core Sandwich Structure and Applied Boundary Conditions.

3.5.3 Basic Experimental Set Ups for the Analysis of the Honeycomb Materials

Two basic experimental apparatuses were used in this analysis. Both consisted of a thin resistance heater positioned between two (nearly) identical samples and either aluminum blocks or insulation placed on the opposite sides of the samples. The edges of the samples were insulated to maintain one dimensional heat transfer. A thermistor was placed on either side of the heater and on the opposite side of the samples in between the sample and the aluminum blocks or insulation to measure temperature. The entire experimental set up was placed in a temperature controlled oven for the experiments. Experiments were conducted at initial temperatures of approximately 295 K, 345 K, 395 K, 445 K, and 495 K, with three repetitions at each temperature for each basic experimental set up; therefore, a total of 30 experiments were conducted. Details of the experimental apparatus can be found in Scott and Copenhaver (1996).

3.5.4 Optimal Experimental Design - Methods

The basic experimental designs described above requires selection of the experimental parameters, including the heating time and the total experimental time. Prior to conducting the experiments, these experimental parameters were optimized to produce temperature measurements which would provide the smallest confidence regions for the estimated thermal properties. Once again, the *D*-criterion was first used, but in addition, a second method was used which sought to minimize the largest confidence interval. This method is called the scaled confidence interval approach and corresponds to maximizing the minimum eigenvalue of the $\boldsymbol{X}^{\mathrm{T}}\boldsymbol{X}$ matrix.

3.6 Estimation of Thermal Properties - Honeycomb Core Structure Results

The results from the analysis of the honeycomb structure included the optimization of the experimental design and the estimation of the thermal properties of composite samples.

3.6.1 Optimal Experimental Design - Results

The first optimal experimental parameter determined was the optimal heating time. The optimal time was first found using the *D*-criterion at temperatures of 295K, 345K, 395K, 445K, and 495K. The specified temperature boundary condition configuration was evaluated first. Here the

optimal heating times ranged from 4560 sec at 295 K to 1500 sec at 495 K. Long heating times were not desired due to the lack of ability to maintain consistent boundary conditions. Therefore, the scaled confidence interval approach was applied as an alternate method. Here it was found that a local minimum could be used without significant loss of information and with a reduction in the experimental time. Therefore, using this approach, the optimal experimental time was found to be 3000 seconds at 295 K, 2000 seconds at 345 K and 395 K, 1690 seconds at 445 K, and 1500 seconds at 495 K. The same procedure was used to find the optimal heating time for the configuration with an insulated boundary away from the heated surface. Here, the recommended heating times were found to be 400 seconds at 295 K, 345 K and 395 K, and 300 seconds at 445 K and 495 K.

The total experimental time was also optimized. The optimal values for the specified temperature boundary condition were found to be 4600 seconds at 295 K, 3300 seconds at 345 K, 3100 seconds at 395 K, 2600 seconds at 445 K, and 2500 seconds at 495 K. The optimal values for the insulated boundary condition case were found to be 1630 seconds at 295 K, 1560 seconds at 345 K, 1500 seconds at 395 K, 1460 seconds at 445 K, and 1400 seconds at 495 K.

3.6.2 Estimation of Thermal Properties

The volumetric heat capacity of the face sheet, the conduction area of the core web, and the emissivity of core cell were the properties sought in the analysis of the honeycomb materials. One concern in this analysis was due to the possible correlation apparent between properties, particularly between the conduction area and the emissivity. The first attempts at estimating these properties using the Box-Kanemasu method resulted in non-convergence; therefore, the Exterior Penalty Function method was used, which resulted in convergence of the parameter estimates.

The results for the mean estimates of the volumetric heat capacity, the conduction area, and the emissivity are shown in Table 6 for both experimental set-ups, along with their respective 95% confidence intervals. Note that the conduction area was expected to be around 3.5×10^{-5} m^2 from actual measurements on a number of samples. The data from the insulated experimental set up were analyzed in two ways. First, the insulation was assumed to be perfect in the mathematical model, and the sensors next to the heater and at the opposite boundary were included in the objective function. Due to the long experimental times however, it was suspected upon looking at the temperature profile at the insulated surface that the insulation at this surface was not perfect. Therefore, the temperature measurements at this boundary were used as specified temperatures in the mathematical model, and the estimation procedure was repeated. The results from both of these cases are shown in Table 6. Note that the specified temperature boundary condition resulted in estimates with overall smaller confidence intervals.

These mean estimates were used in the mathematical model and the resulting temperatures were compared with the experimental results at 295 K and 495 K. The root mean squared error (RMS) as a percentage of the total temperature rise was calculated for the specified temperature and the insulated experimental set ups at both of these temperatures. The mean estimates from the specified temperature experiments provided RMS values of 3.0% at 295 K and 13.9% at 495 K, while the mean estimates from the insulated case with two sensors provided RMS values of 7.9% at 295 K and 28.1% at 495 K. This provided more indication that the specified temperature boundary condition was a better one to use for the estimation of the properties under consideration.

Table 6. Mean Estimated Volumetric Heat Capacitance, C, Conduction Area, A_c, and emissitivy, ϵ, and Associated 95% Confidence Intervals for Specified Temperature and Insulated Experimental Set Ups.

Experimental Set Up		C (MJ/m^{3}K)	A_c (m^2)	ϵ
Specified temperature set up		2.99 ± 0.11	(0.418 ± 0.042)×10^{-4}	0.88 ± 0.10
Insulated set up	(perfect insulation)	3.72 ± 0.33	(0.391 ± 0.079)×10^{-4}	0.50 ± 0.11
	(imperfect insulation)	2.63 ± 0.13	(0.576 ± 0.098)×10^{-4}	0.93 ± 0.05

3.7 Thermal Contact Resistance

Imperfect contact between two adjacent structural components can cause discontinuities in temperature across the two components. These discontinuities can be characterized through the determination of the contact resistance between the two materials. The procedure proposed for the determination of contact resistance is similar to that described for the estimation of thermal properties. In this case, the least squares function is minimized with respect to the contact resistance. In addition, the mathematical model used to provide the calculated temperatures will be modified. For example, the governing differential equations for the mathematical model of the one dimensional system can be described as

$$\frac{\partial}{\partial x}\left(k_{A\text{-}eff}\frac{\partial T_A}{\partial x}\right) = C_{A\text{-}eff}\frac{\partial T_A}{\partial t} \qquad 0 < x < L_A^{+} \qquad t > 0 \qquad (18a)$$

$$\frac{\partial}{\partial x}\left(k_{B\text{-}eff}\frac{\partial T_B}{\partial x}\right) = C_{B\text{-}eff}\frac{\partial T_B}{\partial t} \qquad L_A^{-} < x < L_B \qquad t > 0 \qquad (18b)$$

where L_A and L_B are the thicknesses of the lower and upper plates, respectively, and L_A^{+} and L_A^{-} represent the location on either side of the contact interface. The temperature discontinuity at the interface can be described by the contact resistance, h_c:

$$q = h_c\left(T_{L_A^{+}} - T_{L_A^{-}}\right) \qquad (19)$$

where q is the heat flux at the interface.

A program was written using EAL to estimate the contact resistance between two adjacent samples. Preliminary analysis indicates that this approach has good potential in estimating contact resistance and needs further investigation, including experimentation.

3.8 Use of Genetic Algorithms in Experimental Design Optimization

Due to the tedious nature of the parametric studies performed to optimize the experimental designs used in the estimation of the thermal properties and the difficulties encountered in the simultaneous estimation of correlated properties, alternate methods were sought for the minimization of the objective function in each case. Since the use of derivatives resulted in problems in each of these situations, a non-derivative based method was sought. Genetic algorithms provide for the minimization of an objective function using a probabilitistic directed search without the use of derivatives and were investigated for use in this study.

Genetic algorithms are based on the principle that each technical problem can be translated into an equivalent genetic one which can be optimized by means of biological rules. The advantages are that it can be universally applied and that no prerequisites are required. Also, genetic algorithms have been shown to avoid local optima thus increasing the chance to obtain global optima (Krottmaier, 1993; Doyle, 1995). These algorithms, developed by Holland (1975), are based on genetic and selection mechanisms of nature. Even though they are based on the law of coincidence, they show a steep gradient with regard to improvements (Krottmaier, 1993). Easily programmed, they require no prerequisites or assumptions regarding continuity in the search area. Nevertheless, they have not been widely accepted for engineering applications. This comes from the complexity associated with the use of traditional binary coding. However, the recent demonstrations with both integer and real number codings show promise for other applications (e.g., in structural optimization, Furuya and Haftka, 1993, and in the location of cracks, Doyle, 1995).

In this initial investigation, the objective was to test the proposed optimization strategy based on a basic elitist genetic algorithm on two optimal design problems previously solved in earlier phases of this overall research effort. The first case investigated was the optimization of sensor location and heating time for the simultaneous estimation of two thermal properties of a composite material. This case is described in Sections 3.1.4 and 3.2.1 and in the progress report by Scott and Moncman (1994). The second case was the two dimensional study described in Sections 3.3.4 and 3.4.1 and in the progress report by Scott and Hanak (1995).

3.8.1 Basic Elitist Genetic Algorithm

The basic elitist genetic algorithm employed here was modeled after the algorithm described by Furuya and Haftka (1993). Unlike some traditional optimization techniques that work in the neighborhood of a design point, this algorithm operated on a population of designs, and it involved successive operations consisting of *selection*, *crossover* and *mutation*, which simulated the mechanics of natural genetics. A simplified flowchart of the algorithm is shown in Fig. 3.

In the one-dimensional experiment, a chromosomal string describing a particular design contained two chromosomes for x_s^+ and t_h^+. In the same logic, in the two-dimensional experiments, each string contained four chromosomes for the design variables x_s^+, y_s^+, L_p^+ and t_h^+. Because the design variables were continuous, this modified algorithm used real string representation. The ranges of these variables were bounded by physical as well as practical experimental constraints. The optimization algorithm was initiated by generating the initial parent population of n_s candidate strings (designs). Each string was created by randomly selecting n_c chromosome values (design variable) from the design space. The strings were then ranked in terms of the value of D^+.

Once the initial population was generated, the *selection* operation began as follows. Parents were selected by pairs for breeding using a rank-based fitness technique. The fitness of the I th ranked string was defined as $f_i = n_s + 1 - I$, allowing for the high ranked string to have a high fitness parameter and to be the most likely contribute to the determination of the next generation strings. The probability of the I th ranked string to be selected as a parent was given by $p_i = 2f_i/n_s(n_s+1)$. The selection process was then accomplished at random: the I th ranked string was selected if $P_{i-1} \le r \le P_i$, where r was a uniformly distributed random number between zero and one, and $P_i = \sum_{j=1}^{i-1} P_j$.

The *crossover* operation was completed next. The child strings were made by the mating of the pairs of parents selected for breeding. This process began by generating a random integer k, the cut-off point, between 1 and n_c-1, where n_c was the number of chromosomes. A child was designed by using the first k chromosomes of parent 1 and the remainder from parent 2. In the one-dimensional analysis, consider the strings with $x_s^+ = 0.5$, $t_h^+ = 1.0$ and $x_s^+ = 0.7$, $t_h^+ = 1.5$ as parents 1 and 2, respectively. As $n_c = 2$, the only possible child string is $x_s^+ = 0.5$, $t_h^+ = 1.5$. This process is called single-point crossover. Note that there exists more elaborated variants of this operation which could be more efficient with real number coding.

Finally, *mutation* was implemented by changing at random the value of a chromosome. This process insured that new chromosomes were generated, thus preventing the solution from locking on a non-optimum value. The mutation probability p_m is usually small ($0.001 \le p_m < 0.15$) so as not to interfere with the combination of the best features of parents made by the *crossover* operation. In this work, p_m was taken arbitrarily as 0.05. If the chromosome was mutated, it was replaced by another one randomly chosen from the allowable range of values for that chromosome.

When the operations of *selection*, *crossover* and *mutation* were completed on the n_s parent population, a new generation was created from the n_s-1 child strings in addition to the best parent string. This denotes the basic elitist strategy. Over the course of several generations, n_g, the algorithm tended to converge on the string giving the maximum D^+, which was hence considered as the predicted optimal design. Note that here the number of function evaluations, f_{eval}, can be determined from $f_{eval} = n_s \times (n_g+1)$.

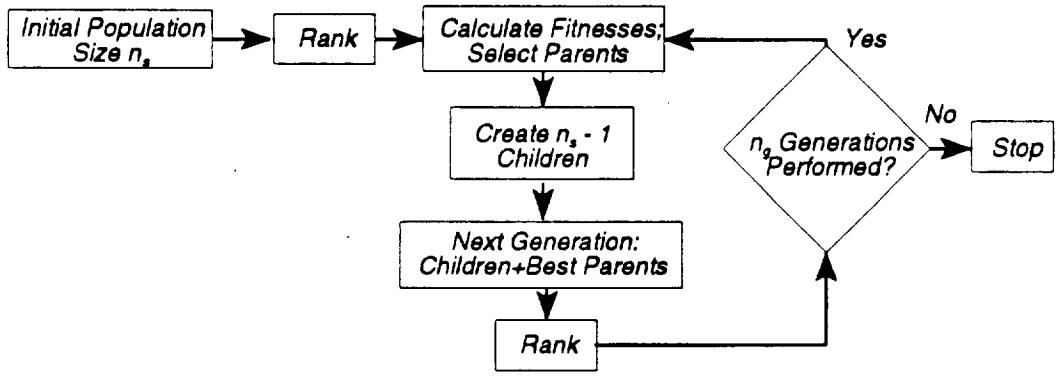

Figure 3. Flow Chart for the Optimization Code Based on a Basic Elitist Genetic Algorithm.

3.8.2 Optimization of Experiments using Genetic Algorithms - Results

The performance of the genetic algorithm was evaluated for the two optimal experimental design problems described previously. The jobs were run on Virginia Tech College of Engineering's Silicon Graphics Power Challenge XL server. In each case, an initial investigation of the effect of the genetic parameters was carried out. The performance of the algorithm was evaluated by averaging ten runs, with the means and their 95-percent confidence intervals calculated for the maximum determinant and each design variable. The means were then compared to the optimal determinants and experimental parameters found by in previous studies. (See Sections 3.2.4 and 3.5.1, Scott and Moncman (1994) and Scott and Hanak (1995)).

3.8.2.1 Results from the One Dimensional Analysis

In the one-dimensional analysis, the design variables to be optimized were x_s^+ and t_h^+. The ranges used for each design variable were identical to those used by Moncman. The effect of both the population size n_s and the number of generations n_g were first analyzed to decide which combination should be utilized in determining the optimal design. In this analysis, the impact of the computing time (or of the number of function evaluations f_{eval}) was not investigated because the dimensionless determinant, D^+, was very inexpensive to calculate. From Table 7, one can see that the maximum D^+ was obtained for the combination with both the largest n_s and n_g (case d), as logically expected. Because the computing time was inexpensive, the combination chosen was the one with the largest n_s and n_g that gave the maximum determinant.

Table 8 shows the results of the ten optimization runs performed using the combination of n_s and n_g discussed above. One result is particularly important: the mean of the maximum D^+ is higher than the maximum D^+ found by Moncman using the parametric study. This ensures that optimal experimental parameters have been obtained and allows for the validation of the optimization procedure based on genetic algorithms. The final optimal experimental parameters should be taken as their respective mean values rounded to the most physically possible values. This would give x_s^+=0.0, and t_h^+=2.29 for the optimal experimental design. These values are actually very close to the optimal parameters given by Moncman (x_s^+=0.0 and t_h^+=2.20).

Table 7. Effect of the Population Size n_s and the Number of Generations n_g in the One-dimensional Experiment.

Case	f_{eval}	n_s	n_g	x_s^+	t_h^+	$D^+_{max}(10^{+2})$
a	2550	50	50	0.0054	2.13	1.9643
b	10200	200	50	0.0019	2.32	1.9856
c	10050	50	200	0.0017	2.44	1.9810
d	40200	200	200	0.0002	2.24	1.9899
Best	40200	200	200			

Table 8. Determination of the Optimal Design for the One-dimensional Experiment (n_s=n_g=200, f_{eval}=40200).

Exp.	x_s^+	t_h^+	$D^+_{max}(10^{+2})$
1	0.0007	2.21	1.9877
2	0.0006	2.33	1.9896
3	0.0015	2.25	1.9838
4	0.0001	2.33	1.9919
5	0.0002	2.24	1.9899
6	0.0005	2.32	1.9911
7	0.0012	2.24	1.9853
8	0.0007	2.31	1.9899
9	0.0002	2.33	1.9914
10	0.0005	2.32	1.9909
Mean	0.0006 ± 0.0003	2.29 ± 0.04	1.9892 ± 0.0019
Moncman's	0.0000	2.20	1.9878

Table 8 also outlines a general feature of genetic algorithms, which is that in the analysis, significant parameters cannot be distinguished from non-significant ones. Consider experiments 4 and 5: even though the sensor locations are almost equal, experiment 4 has still a comparatively much higher D^+. This indicates the importance of the sensor location in the optimal design.

The demonstration of the genetic algorithm on the one-dimensional problem provided a good basis to gain confidence in the algorithm. It also showed that when the objective function is inexpensive to calculate, the genetic algorithm method does not have any computation time restriction (relatively to the number of design variables to optimize). The parametric study, however, requires the analysis of every point in the search space, and thus generally time consuming even for inexpensive objective functions.

3.8.2.2 Results from the Two Dimensional Analysis

In the two-dimensional analysis, two configurations were investigated in which four design variables were optimized. Recall that these latter were x_s^+, y_s^+, t_h^+ and L_p^+. The design variables were expected not to all have the same effect on D^+_{max}. Since x_s^+ was anticipated to have the largest influence on D^+_{max}, the two-dimensional analysis was conducted in two phases. Phase one was performed with a coarse combination of n_s and n_g, which required a low CPU time (~25 min), using the design variable ranges employed by Hanak. The objective was to obtain insight on the relative importance of each design variable. The first phase allowed for both configurations to fix the optimal value of x_s^+ equal to zero so that only three variables needed to be optimized in Phase 2, and

it also allowed to narrow the bounds of the variables to $L_p^+ \geq 0.5$ and $0.9 \leq t_h^+ \leq 3.1$ for Configuration 1 and $1.0 \leq t_h^+ \leq 3.0$ for Configuration 2.

Phase two was managed in a similar manner as the analysis carried out for the one dimensional problem: first, the effect of both n_s and n_g were studied; then the combination chosen for these genetic parameters was used to perform ten optimization runs. The study of n_s and n_g resulted in the use of $n_s = 125$ and $n_g = 50$ for both configurations. Note that increasing n_g to 125 increased the D^+_{max} by 0.3% while the CPU time (and consequently f_{eval}) more than doubled. Thus, since the computation of D^+_{max} was expensive in this case, the values of n_s and n_g providing a slightly less than optimum D^+_{max} were used.

The results for the mean and 95% confidence interval resulting from ten runs for each configuration were compared with the results by Hanak and are shown in Table 9. Again, the means of the D^+_{max}'s from this study are higher than the D^+_{max} 's found by Hanak using the parametric study. These results definitely confirm the assessment of the optimization procedure based on genetic algorithms. Selecting the optimal experimental parameters as their respective means rounded to the closest physically possible values, the optimal design for Configuration 1 gave x_s^+=0.0, y_s^+=0.86, L_p^+=1.0, and t_h^+=1.39; for Configuration 2, it gave x_s^+=0.0, y_s^+=0.0, L_p^+=0.14, and t_h^+=1.40. These values are very close to the optimal experimental parameters determined by Hanak (x_s^+=0.0, y_s^+=0.86, L_p^+=1.0, and t_h^+=1.36 for Configuration 1; x_s^+=0.0, y_s^+=0.0, L_p^+=0.14, and t_h^+=1.41 for Configuration 2).

Note also, that even though the costs associated with the genetic algorithm operations had a small impact on the overall computational costs, it is still of interest to study the diverse effects of using a more elaborated crossover operation, varying the mutation probability and enhancing the elitist strategy of the algorithm. Indeed, both the use of the best combination of the crossover operation and mutation probability, and the enhancement of the elitist strategy of the algorithm could be a means to reduce the population size and/or number of generations, thus reducing the computation time (and number of function evaluations), and still perform as well. These effects are currently under investigation.

Table 9. Determination of the Optimal Designs for Configurations 1 and 2 of the Two-dimensional Experiment (Phase 2, n_s=125, n_g=50, f_{eval}=6375).

Experiment		y_s^+*	L_p^+	t_h^+	$D^+_{max}(10^{+7})$
Conf. 1	Mean	0.860± 0.001	0.995± 0.003	1.39± 0.01	5.383± 0.018
	Hanak's	0.860	1.000*	1.36	5.378
Conf. 2	Mean	0.0008± 0.0004	0.139± 0.001	1.40± 0.01	5.265± 0.013
	Hanak's	0.000	0.140	1.41	5.257

* for L_p^+=1.0, the problem is symmetric (flux applied across the entire boundary)

3.8.3 Conclusions and Future Work

The focus of this paper was on the use of genetic algorithms with real number coding for designing optimal experiments used to estimate thermal properties. The performance of the optimization procedure based on a basic elitist genetic algorithm was demonstrated on both one- and two-dimensional optimal experimental designs previously analyzed, i.e., Scott and Moncman (1994) and Scott and Hanak (1995), respectively, using the most typically applied method in this field, the parametric study. The optimal criterion used in both analysis was the well-known D-criterion. It was found that the genetic algorithm method improved the maximization of the objective function specified by the D-criterion for both test problems. However, from the one-dimensional analysis, it was concluded that the use of the basic elitist genetic algorithm did not allow for the distinction between significant and non-significant parameters. Therefore, the optimization of the two-dimensional problem was conducted in two phases, the first enabling insight to be obtained on the significance of each parameter to be optimized. Furthermore, on one hand it was shown that when the objective function was inexpensive to calculate, as in the one-dimensional analysis, the genetic algorithm method reduced considerably the computation costs over the parametric study; on the other hand, when the objective function was highly expensive to calculate, as in the two-dimensional analysis, due to the need to average the performance of the algorithm over several runs, the genetic algorithm method tended to be as time intensive as the parametric study, although less tedious to apply.

Present work involves the development of an extended elitist genetic algorithm that has shown not only to perform better than the basic elitist genetic algorithm on the cases studied here, but also to be an effective strategy for the simultaneous estimation of correlated parameters.

4. PUBLICATIONS AND THESIS

The following publications and theses have been completed with support from this grant. Note that this listing includes only completed works and not those in progress.

4.1 Publications

Garcia, S., and E. P. Scott, 1996, "Use of Genetic Algorithms in Optimal Experimental Designs," accepted for presentation at and publication in the proceedings of the 2nd International Conference on Inverse Problems in Engineering: Theory and Practice, June 9-14, Port aux Rocs, Le Croisic, France.

Scott, E. P. and R. T. Haftka, 1995, "Optimization and Experiments," *AIAA No. 95-0121*, pp.1-11.

Moncman, D. A., J. P. Hanak, D. C. Copenhaver, and E. P. Scott, 1995, "Optimal experimental designs for estimating thermal properties," paper presented at and published in the proceedings of the 4th American Society Mechanical Engineers - Japanese Society of Mechanical Engineers Thermal Engineering Joint Conference, Maui, HI, Vol. 3, pg. 461-468.

4.2 Completed Thesis

Copenhaver, D. C., 1996, *Thermal Characterization of Honeycomb Core Sandwich Structures*, M.S. Thesis, Department of Mechanical Engineering, Virginia Tech, Blacksburg, VA.

Hanak, J. P., 1995, *Experimental Verification of Optimal Experimental Designs for the Estimation of Thermal Properties of Composite Materials*, M.S. Thesis, Department of Mechanical Engineering, Virginia Tech, Blacksburg, VA.

Moncman, D. A., 1994, *Optimal Experimental Designs for the Estimation of Thermal Properties of Composite Materials*, M.S. Thesis, Department of Mechanical Engineering, Virginia Tech, Blacksburg, VA.

5. REFERENCES

Beck, J. V. and K. J. Arnold, 1977, *Parameter Estimation in Engineering and Science*, John Wiley & Sons, New York.

Doyle, J. F., June 12-13, 1995, "Determining the Size and Location of a Crack in a Frame Structure," *Proceedings of the Seventh Inverse Problems in Engineering Seminar*, OSU.

Furuya, H. and R. T. Haftka, July 17-22, 1993, "Genetic Algorithms for Placing Actuators on Space Structures," *Proceedings of the Fifth International Conference on Genetic Algorithms*, Urbana, IL., pp. 536-542.

Holland, J. H., 1975, *Adaptation of Natural and Artificial Systems*, The University of Michigan Press, Ann Arbor, MI.

Krottmaier, J., 1993, *Optimizing Engineering Designs*, McGraw-Hill Book Company, London.

Scott, E. P. and D. C. Copenhaver, 1996, *Thermal Characterization of Honeycomb Core Sandwich Structures*, Progress Report for NASA Contract No. NAG-1-1507, Virginia Tech, Blacksburg, VA.

Scott, E. P. and R. T. Haftka, 1995, "Optimization and Experiments," *AIAA No. 95-0121*, pp.1-11.

Scott, E. P., and J. P. Hanak, 1995, *Experimental Verification of Optimal Experimental Designs for the Estimation of Thermal Properties of Composite Materials*, Progress Report for NASA Contract No. NAG-1-1507, Virginia Tech, Blacksburg, VA.

Scott, E. P., and D. A. Moncman, 1994, *Optimal Experimental Designs for the Estimation of Thermal Properties of Composite Materials*, Progress Report for NASA Contract No. NAG-1-1507, Virginia Tech, Blacksburg, VA.

Whetstone, W.D., 1983, *EISI-EAL Engineering Analysis Language*, Engineering Information Systems, Inc., San Jose, CA.